

# RF MEMS in Wireless Architectures

Clark T.-C. Nguyen  
DARPA/MTO

3701 North Fairfax Drive, Arlington, Virginia 22203-1714  
(On leave from the University of Michigan, Ann Arbor, Michigan 48109-2122)  
1-571-218-4586

cnguyen@darpa.mil

## ABSTRACT

Micromechanical (or “ $\mu$ mechanical”) communication circuits fabricated via IC-compatible MEMS technologies and capable of low-loss filtering, mixing, switching, and frequency generation, are described with the intent to miniaturize wireless transceivers. Possible MEMS-based receiver front-end architectures are then presented that use these micromechanical circuits in large quantities to enhance robustness and substantially reduce power consumption. Among the more aggressive architectures proposed are one based on a  $\mu$ mechanical RF channel-selector and one featuring an all-MEMS RF front-end.

## Categories and Subject Descriptors

B.7.1: [Integrated Circuits]: Types and Design Styles --- *advanced technologies*

## General Terms

Design, Experimentation.

## Keywords

RF MEMS, quality factor, micromechanical circuit, RF front end, resonator, switch, inductor, capacitor

## 1. INTRODUCTION

Recent demonstrations of micro-scale high- $Q$  passive components that utilize microelectromechanical systems (MEMS) technology to allow on-chip integration alongside transistor circuits have sparked a resurgence of research interest in communication architectures that emphasize the use of high- $Q$  passive devices [1]-[4]. Among the most useful of these are  $\mu$ mechanical RF switches with insertion losses as low as 0.1dB [5]; tunable  $\mu$ mechanical capacitors with  $Q$ 's up to 300 at 1 GHz [6][7];  $\mu$ machined inductors with  $Q$ 's up to 70 at 1 GHz [8]; and vibrating micromechanical (“ $\mu$ mechanical”) resonator circuits with frequencies spanning a few kHz to several GHz, and with  $Q$ 's in the tens of thousands [9]-[14]—all achieved in orders of magnitude smaller size than macroscopic counterparts, and with little or no power consumption. Although much of the interest in these “RF MEMS” devices originally derived from their amenability to on-chip integration, it

is actually their potential for enhancing robustness and reducing power consumption in alternative transceiver architectures that makes them so compelling. This brief review paper aims to convey some of the more compelling arguments for their use in future RF systems.

## 2. MICROMECHANICAL RF DEVICES

Table 1 summarizes some of the more popular RF MEMS devices in each of the categories mentioned above. Each device is now briefly described.

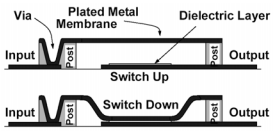
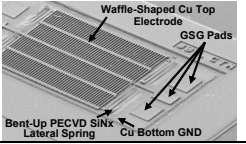
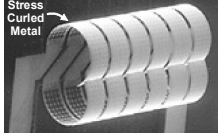
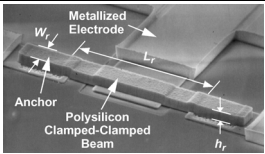
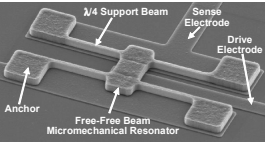
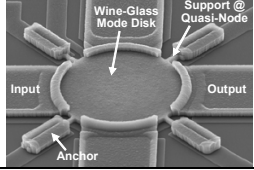
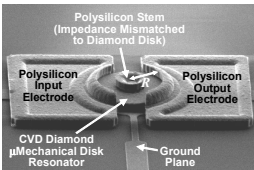
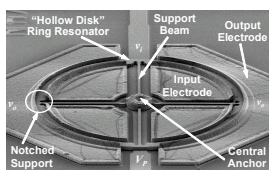
### 2.1 Micromechanical Switches

With typical insertion losses as low as 0.1dB, third-order input intercept points  $IIP_3$  greater than 66dBm, and picowatts per switch power consumption, micromechanical switches [5] can greatly outperform semiconductor switches (FETs or diodes) in antenna and filter switching applications. They achieve such impressive performance characteristics by virtue of their micromechanical construction, which not only provides a mechanical operation mechanism much like that of macroscopic mechanical switches, but further allows the use of metal materials with substantially lower resistivity than semiconductors. The specific switch in row 1 of Table 1 essentially comprises a beam fixed at both ends and suspended over a metal electrode (that could be the center conductor of a coplanar waveguide). When sufficient voltage is applied between the beam and its underlying electrode, the ensuing electrostatic force pulls the beam down to the electrode, shorting the two (for the case of a direct contact switch), or raising the electrode-to-beam capacitance to affect an ac short (for a capacitive switch, where a dielectric film sits atop the electrode); in either case, effectively closing the switch. For the popular case of electrostatic actuation, voltage levels  $>20V$  are common for radar applications. This actuation voltage level, however, is too high for the integrated transistor circuits used in wireless handset applications, so must either be lowered, or otherwise accommodated (e.g., via charge pumping) at the system-level.

When designed with length dimensions on the order of 100  $\mu m$ , achievable micromechanical switching speeds on the order of microseconds are much slower than that of FETs. Although nanosecond switching speeds are likely feasible with smaller dimensions, the microsecond speeds already demonstrated are quite adequate for the many switching applications in wireless subsystems for which low loss and high linearity are paramount. These include: (1) antenna switching and programmable low-loss filtering for multi-band reconfigurability and diversity against multi-path fading; (2) antenna steering, e.g., via a phased array approach; and (3) power amplifier (PA) supply switching for reduced PA power consumption.

Copyright 2005 Association for Computing Machinery. ACM acknowledges that this contribution was authored or co-authored by a contractor or affiliate of the U.S. Government. As such, the Government retains a nonexclusive, royalty-free right to publish or reproduce this article, or to allow others to do so, for Government purposes only.  
DAC 2005, June 13–17, 2005, Anaheim, California, USA.  
Copyright 2005 ACM 1-59593-058-2/05/0006...\$5.00.

**Table 1: Summary of RF MEMS Devices**

De-vice	Photo	Performance	Applications	Research Issues
$\mu$ Mechanical Switch [5]		Demonstrated: $IL \sim 0.1$ dB, $IIP_3 \sim 66$ dBm Switching Voltage: $>20$ V Switching Time: $\sim 5$ $\mu$ s trade switching voltage vs. power handling and isolation	Tunable Biasing Tunable Matching Phase Array Antennas Multi-Band RF Filter?	reliability switching voltage switching speed hot switching
Tunable Capacitor [7]		Demonstrated: $Q \sim 300$ @ 1 GHz using movable dielectric $Q$ lower w/ movable metal plate Capacitance: 1-4 pF	$>$ UHF VCO's Tunable Biasing Tunable Matching Multi-Band RF Filter	tuning range stress control packaging microphonics
$\mu$ Mechanical Inductor [8]		Demonstrated: $Q \sim 70$ @ 1 GHz over low-resistance silicon using out-of-plane stressed-curved metal $Q$ Range: can it get to 300?	$>$ UHF VCO's Biasing/Matching Multi-Band RF Filter?	$Q$ must increase to 300 for multi-band filter microphonics
CC-Beam Resonator [9]		Demo'ed: $Q \sim 8,000$ @ 10 MHz (vac) $Q \sim 50$ @ 10 MHz (air) $Q \sim 300$ @ 70 MHz (anchor diss.) $Q$ drop w/ freq. limits freq. range Series Resistance, $R_x \sim 5$ -5,000 $\Omega$	Reference Oscillator HF-VHF Filter HF-VHF Mixer-Filter (arrays of the above)	power handling thermal/aging stability impedance vacuum packaging
FF-Beam Resonator [10]		Demo'ed: $Q \sim 20,000$ from 10-200 MHz $Q \sim 2,000$ @ 90 MHz (air) No drop in $Q$ with freq. Freq. Range: $>1$ GHz; unlimited w/ scaling and use of higher modes Series Resistance, $R_x \sim 5$ -5,000 $\Omega$	Reference Oscillator HF-UHF Filter HF-UHF Mixer-Filter Ka-Band? (arrays of above)	freq. extension power handling thermal/aging stability impedance vacuum packaging
Wine-Glass Disk Res. [11]		Demo'ed: $Q \sim 156,000$ @ 60 MHz (vac) $Q \sim 8,000$ @ 98 MHz (air) Perimeter support design nulls anchor loss to allow extremely high $Q$ Freq. Range: $>1$ GHz; unlimited w/ scaling Series Resistance, $R_x \sim 5$ -5,000 $\Omega$	Reference Oscillator HF-UHF Filter HF-UHF Mixer-Filter (arrays of the above)	freq. extension power handling thermal/aging stability impedance
Contour-Mode Disk Res. [13]		Demo'ed: $Q \sim 11,555$ @ 1.5 GHz (vac) $Q \sim 10,100$ @ 1.5 GHz (air) Balanced design and material mismatching anchor-disk design nulls anchor loss Freq. Range: $>1$ GHz; unlimited w/ scaling and use of higher modes Series Resistance, $R_x \sim 50$ -50,000 $\Omega$	RF Local Oscillator VHF-S-Band Filter VHF-S-Band Mixler Ka-Band? RF Channel-Select (arrays of above)	thermal/aging stability impedance Xmit power handling
Hollow Disk Ring Res. [14]		Demo'ed: $Q \sim 14,600$ @ 1.2 GHz (vac) $\lambda/4$ support design nulls anchor loss Freq. Range: $>1$ GHz; unlimited w/ scaling and use of higher modes Series Resistance, $R_x \sim 50$ -5,000 $\Omega$	RF Local Oscillator UHF-S-Band Filter UHF-S-Band Mixler Ka-Band? RF Channel-Select (arrays of above)	thermal/aging stability impedance Xmit power handling

For some time, the adaptation of micromechanical RF switches had been hindered by reliability concerns, since early switches had lifetimes on the order of only 10 million cycles, after which they failed by either sticking down or developing a permanent open (e.g., via growth of a dielectric material over the contact surfaces). Today, however, a combination of contact engineering, proper packaging, and manufacturing control, now make available RF MEMS switches capable of switching over 100 billion cycles. This is more than enough for the vast majority of commercial and

military applications, and now clears a path for greater acceptance of these devices into mainstream wireless markets.

## 2.2 Medium- $Q$ Tunable Capacitors

Tunable  $\mu$ mechanical capacitors, summarized in row 2 of Table 1, consist of either metal plates that can be electrostatically moved with respect to one another, allowing voltage-control of the capacitance between the two plates; or dielectrics that can be electrostatically positioned between two metal plates to again allow voltage control of the plate-to-plate capacitance. As with switches,

because metal materials can be used in their construction,  $Q$ 's as high as 300 can be attained [7]—much higher than attainable by the lossy semiconductor pn diodes offered by conventional IC technology. Paired with medium- $Q$  inductors,  $\mu$ mechanical capacitors can enhance the performance of low noise VCO's. Also, if inductors could be achieved with  $Q$ 's as high as 300, tunable RF pre-select filters might be attainable that could greatly simplify the implementation of multi-band transceivers.

### 2.3 Medium- $Q$ Micromachined Inductors

As mentioned above, tunable  $\mu$ mechanical capacitors must be paired with inductors with  $Q > 20$  to be useful in communication circuits. Unfortunately, due to excessive series resistance and substrate losses, *conventional* IC technology can only provide spiral inductors with  $Q$ 's no higher than 7. Using MEMS technologies to both thicken metal turns (reducing series resistance) and suspend the inductor turns away from the substrate (reducing substrate losses), inductors with  $Q$ 's as high as 70 at 1 GHz have been demonstrated (c.f., row 3 of Table 1) [8]. Although not the  $Q \sim 300$  needed for multi-band tunable RF filters, this  $Q \sim 70$ , when paired with a  $\mu$ mechanical capacitor, should allow the implementation of low noise VCO's with much lower power consumption than those using conventional IC technology [15]. Tunable bias/matching networks that can reduce power consumption in power amplifiers should also be feasible.

### 2.4 High- $Q$ Vibrating Micromechanical Resonators

Because mechanical resonances generally exhibit orders of magnitude higher  $Q$  than their electrical counterparts, vibrating mechanical resonators are essential components in communication circuits. With appropriate scaling via MEMS technology, such devices can be designed to vibrate over a very wide frequency range, from  $<1$  kHz to  $>1$  GHz, making them ideal for ultra stable oscillator and low loss filter functions for a wide range of transceiver types.

The last 5 rows of Table 1 succinctly present the evolution of vibrating  $\mu$ mechanical resonator geometries over the past 8 years. As shown, clamped-clamped beam resonators, which are essentially guitar strings scaled down to micron dimensions to achieve VHF frequencies, can achieve on-chip  $Q$ 's  $\sim 8,000$  for oscillator and filtering functions in the HF range. However, anchor losses in this specific structure begin to limit the achievable  $Q$  at higher VHF frequencies, limiting the practical range of this structure to  $<100$  MHz when using  $\mu$ m-scale dimensions. To achieve higher frequency while retaining  $Q$ 's in the thousands and without the need for sub- $\mu$ m dimensions [16] (which can potentially degrade the power handling and frequency stability of these devices in present-day applications [17]), more balanced structures that eliminate anchor losses can be used, such as the free-free beam [10] of row 5, the compound (2,1)- and radial-mode disk resonators in rows 6 and 7, or the extensional ring resonator of row 8, in Table I. As shown, these resonators operate at and beyond GHz frequencies when properly scaled, and do so while retaining sufficiently large dimensions to maintain adequate power handling and avoid "scaling-induced" phenomena, such as mass-loading or temperature fluctuation noise, that can begin to degrade performance when dimensions become too small [17].

Focusing in on one of the devices, the radial contour mode micromechanical disk resonator in row 7 attains a second-mode frequency of 1.51 GHz with a  $Q$  of 11,555 in vacuum, and 10,100 in air (i.e., at atmospheric pressure), while still retaining relatively large dimensions. This device consists of a 20 $\mu$ m-diameter, 2 $\mu$ m-thick doped-CVD diamond disk suspended by a doped-polysilicon stem self-aligned to be exactly at its center, all enclosed by doped-polysilicon electrodes spaced 80nm from the disk perimeter. When vibrating in its radial contour mode, the disk expands and contracts around its perimeter in what effectively amounts to a high stiffness, high energy, extensional-like mode. Since the center of the disk corresponds to a node location for the radial contour vibration mode shape, anchor losses through the supporting stem are greatly suppressed, allowing this design to retain a very high  $Q$  even at this UHF frequency. In addition, the high stiffness of its radial contour mode gives this resonator a much larger total (kinetic) energy during vibration than exhibited by previous resonators, making it less susceptible to energy losses arising from viscous gas damping, hence, allowing it to retain  $Q$ 's  $>10,000$  even at atmospheric pressure. This single resonator not only achieves a frequency applicable to the RF front ends of many commercial wireless devices, it also removes the requirement for vacuum to achieve high  $Q$ , which should greatly lower the cost of this technology.

Although the vibrating resonator devices presented in Table 1 all utilize capacitive transduction, versions of such resonators have also been realized using piezoelectric [18] and magnetomotive methods [16]. The choice of transduction method greatly impacts not only the achievable  $Q$  and impedance of these devices, but also their amenability to integration and design automation. In particular, although the more efficient electromechanical coupling factor of a piezoelectric transducer can help to reduce the impedance of a vibrating resonator, the use of such a transducer often introduces fabrication complexity (hence increases cost), reduces device  $Q$ , and can compromise integration density and amenability to system-level design automation. The last of these, for example, constitutes a significant drawback for piezoelectric FBAR resonators, for which resonance frequency is determined by thickness rather than lateral dimensions, making it difficult to specify multiple frequencies on a single-chip via CAD layout. In contrast, the frequencies of the capacitively-transduced devices in Table 1 are governed by one or more lateral dimensions, allowing a designer to specify a frequency via CAD layout, and more importantly, allowing automated specification of a larger circuit of resonators with varying frequencies, all on a single chip.

### 2.5 Micromechanical Circuits

Although stand-alone vibrating  $\mu$ mechanical resonators are themselves applicable to local oscillator synthesizer applications in transceivers [19][20], their application range can be greatly extended by using them in circuit networks. In particular, by interlinking mechanical elements into specific networks, a variety of low-loss circuit functions are available, from bandpass filters [9] to mixers [21] to gain devices [22]. **Fig. 1** presents the scanning electron micrograph (SEM) and measured frequency characteristic for a 68.1-MHz polysilicon surface-micromachined  $\mu$ mechanical filter that occupies an area of only 250 $\mu$ m $\times$ 60 $\mu$ m, and that shows  $<2.7$ dB of insertion loss for a 0.28% bandwidth, all attained with zero dc power consumption [23]. Furthermore, the use of capacitive transduction by this filter makes it on/off switchable via mere

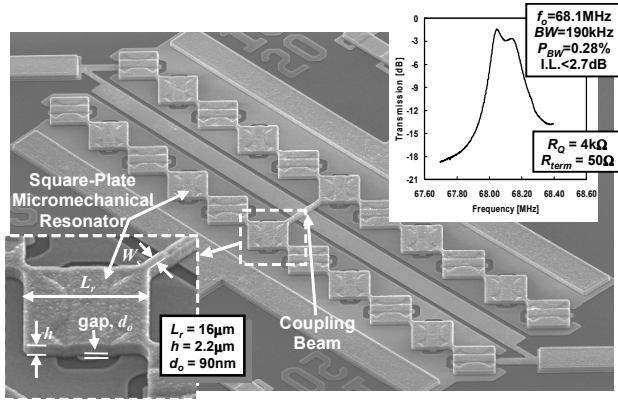


**Fig. 1: SEM of a 68.1-MHz micromechanical bandpass filter using mechanically-coupled square-plate resonator array composite resonators to lower its input/output impedance.**

charging and discharging of its conductive vibrating structure, i.e., by mere application and removal of a dc-bias voltage (with no dc current flow, hence no dc power consumption). This is another key advantage of capacitive transduction, since it enables switching of this filter in and out of the transmit or receive path of an RF front end *without the need for series switches*; i.e., without the cost and insertion loss associated with such switches.

Although the use of capacitive transducers has performance and cost advantages over other types, their inefficiency often incurs higher input and output impedances for a given filter. This complicates matching to macroscopic components in wireless circuits, such as antennas, which often require matching to  $50\Omega$  or  $377\Omega$  for maximum power transfer. As mentioned, one way to circumvent this problem is to use piezoelectric transduction. Indeed, laterally vibrating piezoelectric micromechanical resonators with frequencies governed by lateral dimensions (making them CAD compatible) have recently been reported [18] with impedances more in line with the needs of off-chip antennas. Although these devices presently post lower  $Q$  than capacitively-transduced counterparts and use a fabrication flow that requires a greater deviation from standard IC processing than surface-micromachined devices, they do present a reasonable solution to the impedance problem.

Still, because of their higher  $Q$ , process simplicity and IC compatibility [24] (i.e., lower cost), and built-in switchability, surface-micromachined capacitively-transduced resonators are arguably the more preferred, especially considering the greater need for higher  $Q$  and integration with transistors by the wireless architectures to be described in the next section. Fortunately, there are now mechanical circuit design solutions that allow capacitively-transduced devices to achieve much lower impedances. For example, the filter of **Fig. 1** actually achieves a low enough input/output impedance to match to  $50\Omega$  via use of mechanically-coupled arrays of capacitively-transduced square resonators as “composite” end resonators [23]. This arraying approach automatically matches the frequencies of constituent resonators and sums their outputs to generate a larger total current for a given input voltage, thereby lowering the impedance and allowing matching to  $50\Omega$ . The technique is very much akin to the use of transistor arrays in cascaded CMOS digital driver circuits to transform the high impedance of a minimum size logic gate to a lower impedance buffer capable of driving off-chip loads. Perhaps in the

future, the choice between using an array of capacitively-transduced resonators versus a single piezoelectric resonator will be similar to the choice between using a CMOS cascaded buffer versus a bipolar driver?

Whatever the choice, the concept of a micromechanical circuit that combines many on-chip mechanical links to attain a more complex function is reminiscent of the same concept already applied to on-chip transistors to revolutionize electronics today. With 43 resonators and links, the filter of **Fig. 1** already qualifies as a medium-scale integrated (MSI) micromechanical circuit. (And this is just the beginning.)

### 3. MEMS-BASED TRANSCEIVER ARCHITECTURES

Perhaps the most direct way to harness RF MEMS devices is via direct replacement of off-chip components in an existing transceiver architecture, whether it be super-heterodyne or homodyne. Indeed, even just direct replacement of components via MEMS-based ones can lead to significant performance increases. For example, analyses before and after replacement of off-chip high- $Q$  passives by higher  $Q$  MEMS versions in a super-heterodyne architecture often show dramatic improvements in receiver noise figure, e.g., from 8.8 dB to 2.8 dB. In addition, low phase noise oscillators referenced to micromechanical resonator frequency-setting elements have recently been demonstrated with substantially lower power consumption than counterparts using macroscopic resonators [19][20].

Although beneficial, the performance gains afforded by mere direct replacement by MEMS are quite limited when compared to more aggressive uses of MEMS technology. To fully harness the advantages of  $\mu$ mechanical circuits, one should take advantage of their micro-scale size and zero dc power consumption, and use them in massive quantities to enhance robustness and trade  $Q$  for power consumption. **Fig. 2** presents the system-level block diagram for a possible transceiver front-end architecture that takes full advantage of the complexity achievable via  $\mu$ mechanical circuits. The main driving forces behind this architecture are robustness and power reduction, attained in several of the blocks by replacing active components by low-loss passive  $\mu$ mechanical ones, and by trading power for high selectivity (i.e., high- $Q$ ). Among the key performance enhancing features are: (1) an RF channel selector comprised of a bank of switchable  $\mu$ mechanical filters, offering multi-band reconfigurability, receive power savings via relaxed dynamic range requirements [3], and transmit power savings by allowing the use of a more efficient power amplifier; (2) use of passive  $\mu$ mechanical mixer-filters to replace the active mixers normally used, with obvious power savings; (3) a VCO referenced to a switchable bank of  $\mu$ mechanical resonators, capable of operating without the need for locking to a lower frequency reference, hence, with orders of magnitude lower power consumption than present-day synthesizers; (4) use of  $\mu$ mechanical T/R switching (via an RF MEMS switch, or via a network of switchable capacitively-transduced vibrating micromechanical filters, which is shown), with the potential for large power savings in transmit-mode; and (5) use of  $\mu$ mechanical resonator and switch components around the power amplifier to enhance its efficiency.

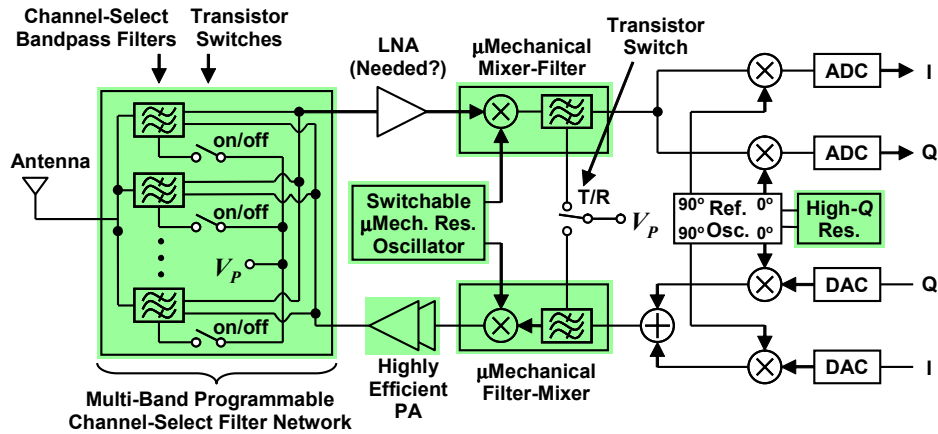


Fig. 2: System-level block diagram for a low-power RF channel-select transceiver architecture that uses RF MEMS devices (shaded) to enhance robustness and lower power consumption over present-day architectures.

Although already quite aggressive, the architecture of Fig. 4 may still not represent the best power savings afforded by MEMS. In fact, even more robustness and power savings than in Fig. 4 are possible if the high- $Q$   $\mu$ mechanical circuits in the signal path can post such low losses that the RF LNA (normally required to boost the received signal against losses and noise from subsequent stages) may in fact no longer be needed. Rather, the RF LNA can be removed, which effectively removes its noise, power consumption, and linearity limitations, resulting in a larger front-end dynamic range. The needed gain to baseband can be provided instead by an IF LNA that consumes much less power, since it operates at the much lower IF frequency.

#### 4. CONCLUSIONS

Micromechanical devices and circuits attained via MEMS technologies have been described that can potentially play a key role in removing the board-level packaging requirements that currently constrain the size of communication transceivers. In addition, by combining the strengths of integrated  $\mu$ mechanical and transistor circuits, using both in massive quantities, previously unachievable functions become possible that may soon enable alternative transceiver architectures with substantial performance gains, especially from robustness and power perspectives. To reap the benefits of these new architectures, however, further advancements in design automation for micromechanical circuits are needed.

#### 5. ACKNOWLEDGMENTS

Much of the work presented was supported by grants and contracts from DARPA and NSF.

#### 6. REFERENCES

- [1] C. T.-C. Nguyen, 2004 IEEE Custom Integrated Ckts. Conf. (CICC), Orlando, Florida, Oct. 3-6, 2004, pp. 257-264.
- [2] C. T.-C. Nguyen, 2000 Bipolar/BiCMOS Ckts. and Tech. Mtg (BCTM), Sept. 25-26, 2000, pp. 142-149.
- [3] C. T.-C. Nguyen, *IEEE Trans. Microwave Theory Tech.*, vol. 47, no. 8, pp. 1486-1503, Aug. 1999.
- [4] C. T.-C. Nguyen, L. P.B. Katehi, and G. M. Rebeiz, *Proc. IEEE*, vol. 86, no. 8, pp. 1756-1768, Aug. 1998.
- [5] Z. J. Yao, *et al.*, *IEEE/ASME J. Microelectromech. Syst.*, pp. 129-134, June 1999.

- [6] D. J. Young, *et al.*, 1996 Solid-State Sensor and Actuator Workshop, June 2-6, 1996, pp. 86-89.
- [7] J.-B. Yoon, *et al.*, 2000 IEEE Int. Electron Devices Meeting (IEDM), Dec. 11-13, 2000, pp. 489-492.
- [8] C. L. Chua, *et al.*, *IEEE/ASME J. Microelectromech. Syst.*, vol. 12, no. 6, pp. 989-995, Dec. 2003.
- [9] F. D. Bannon III, *et al.*, *IEEE J. Solid-State Circuits*, vol. 35, no. 4, pp. 512-526, April 2000.
- [10] K. Wang, *et al.*, *IEEE/ASME J. Microelectromech. Syst.*, vol. 9, no. 3, pp. 347-360, Sept. 2000.
- [11] M. A. Abdelmoneum, *et al.*, *Proceedings*, 2003 IEEE MEMS Conf., Kyoto, Japan, Jan. 19-23, 2003, pp. 698-701.
- [12] J. Wang, *et al.*, *IEEE Trans. Ultrason., Ferroelect., Freq. Contr.*, vol. 51, no. 12, pp. 1607-1628, Dec. 2004.
- [13] J. Wang, *et al.*, 2004 IEEE MEMS Conf., Maastricht, The Netherlands, Jan. 25-29, 2004, pp. 641-644.
- [14] S.-S. Li, *et al.*, 2004 IEEE MEMS Conf., Maastricht, Netherlands, Jan. 25-29, 2004, pp. 821-824.
- [15] A. Dec, *et al.*, *IEEE J. Solid-State Circuits*, vol. 35, no. 8, pp. 1231-1237, Aug. 2000.
- [16] M. L. Roukes, 2000 Solid-State Sensor and Actuator Workshop, June 4-8, 2000, pp. 367-376.
- [17] J. R. Vig, *et al.*, *IEEE Trans. Ultrason. Ferroelec. Freq. Contr.*, vol. 46, no. 6, pp. 1558-1565, Nov. 1999.
- [18] G. Piazza, *et al.*, 2005 IEEE MEMS Conf., Miami, Florida, Jan. 30 – Feb 3, 2005, pp. 20-23.
- [19] Y.-W. Lin, *et al.*, *IEEE J. Solid-State Circuits*, vol. 39, no. 12, pp. 2477-2491, Dec. 2004.
- [20] B. P. Otis and J. M. Rabaey, *IEEE J. Solid-State Circuits*, vol. 38, no. 7, pp. 1271-1274, July 2003.
- [21] A.-C. Wong and C. T.-C. Nguyen, *IEEE/ASME J. Microelectromech. Syst.*, vol. 13, no. 1, pp. 100-112, Feb. 2004.
- [22] J.P. Raskin, *et al.*, *IEEE/ASME J. Microelectromech. Syst.*, vol. 9, pp. 528-537, Dec. 2000.
- [23] M. U. Demirci and C. T.-C. Nguyen, "A Low Impedance VHF Micromechanical Filter Using Coupled-Array Composite Resonators," to be published in the *Technical Digest of TRANSDUCERS'05*, Seoul, Korea, June 5-9, 2005.
- [24] C. T.-C. Nguyen and R. T. Howe, *IEEE J. Solid-State Circuits*, vol. 34, no. 4, pp. 440-455, April 1999.